〈論 文〉 3-4-5

다부하를 갖는 유도가열기기를 위한 고역률 이중 하프브릿지 직렬공진 인버터

鄭 龍 采

High Power Factor Dual Half Bridge Series Resonant Inverter for an Induction Heating Appliance with Multiple Loads

Yong-Chae Jung

요 약

근접부하의 동작주파수의 차이에 의해 발생하는 간섭가청잡음을 제거하기 위해서 다부하를 갖는 유도가열기기를 위한 새로운 고역률 이중 하프브릿지 직렬공진 인버터를 제안한다. 이 회로는 하나의 인버터로 두 개의 유도가열요소를 독립적으로 전대역 출력제어를 할 수 있고 영전압 스위칭 특성 때문에 최소 스위칭 손실을 갖는다. 모드분석을 통해서 제안된 회로의 동작을 설명할 것이다. 요구되는 냉각능력을 평가하기 위해서 몇 개의 손실식을 유도함으로써 손실분석을 행하였다. 역률제어기능을 갖고 시스템의 크기를 축소하기 위해서 적절한 설계가이드를 제시하였다. 이렇게 설계된 값들을 사용하여 각 유도가열요소가 2.8kW 전력소모를 갖는 proto-type 회로를 구성하고 제안된 회로의 동작을 확인하기 위해서 실험을 행하였다.

ABSTRACT

A novel high power factor Dual Half Bridge Series Resonant Inverter (DHB-SRI) for an induction heating appliance with multiple loads is proposed to remove the interferential acoustic noise caused by the difference between operating frequencies of adjacent loads. The circuit enables independent full power range control of two induction heating elements by one inverter circuit and has minimum switching losses due to the zero voltage switching characteristic. According to the mode analysis, I will explain the operation of the proposed circuit. To evaluate the required cooling capacity, loss analysis is performed through deriving some loss equations. In order to obtain the power factor correction capability and to lessen the system size, suitable design guides are given. Using the designed values, the proto-type circuit with 2.8kW power consumption for each induction heating element is built and tested to verify the operation of the proposed circuit.

Key Words: Induction heating, High power factor, Dual half bridge, Series resonant, Multiple loads

1. INTRODUCTION

The induction heating technology is utilized in a wide variety of applications such as heating, welding, hardening, cooking and so on. Since it applied to the home appliance in the mid 1970s, many researches for an induction heating cooker have been intensively carried out.[1~4]

The operational principle of the induction heating cooker is as follows. An inverter circuit forces the high frequency alternating current to flow into a work coil. Then, an alternating magnetic flux passing through a cooking vessel is generated. The magnetic flux induces eddy currents in the bottom of the cooking vessel, and the cooking vessel is heated up by the induced eddy currents.

To make the high frequency alternating current using this principle in the induction heating cooker, there are many kinds of inverter topologies such as the single switch class E type inverter[2, 3], the half bridge series resonant inverter[1, 4] and so on. Among them, the single switch class E type inverter is popular in the power range of less than 1.3kW. To obtain the high power capability, the half bridge series resonant inverter is commonly used.

In the series resonant inverter, the characteristics of the output power according to the operating frequency have the Gaussian-Distribution curves centering at the resonant frequency. Therefore, the above-resonance frequency control method is generally adopted. Using the control method, audible noise can be avoided because the maximum power is obtained at the lower limit of switching frequency more than 20kHz. Thus, the output power varies with the operating frequency in the range of 20kHz to 50kHz.

In some application, it is required to operate more than one induction heating element in the same appliance.[1] In this case, it generally makes use of separate inverters with independent power controls to drive each heating element. However, when adjacent inverters are operated simultaneously, acoustic noises are generated by the difference between operating frequencies of each inverter. To eliminate the acoustic noise, the first available method is that each inverter is controlled using duty control at the same frequency.[1] However, the whole system becomes more complex, bulky and expensive as ever.

Therefore, in order to resolve the above-mentioned problems, a new high power factor Dual Half Bridge Series Resonant Inverter (DHB-SRI) for an induction heating appliance with multiple loads is proposed in this paper. The proposed circuit having a simple inverter structure can get into operation two loads in turn to remove the acoustic noise, and has minimum switching losses on account of the zero voltage switching feature. The mode analysis of the DHB-SRI is performed to illustrate the circuit operation. In addition, the loss equations for main loss generating parts are derived to evaluate the required cooling capacity. To lessen the system size and to obtain the high power factor correction, the proper design method of filter components is given. Also, the design procedures of resonant components are presented. The proto-type DHB-SRI with 2.8kW power consumption for each induction heating element is built and tested to verify the operation of the proposed circuit.

2. THE PROPOSED DHB-SRI

The proposed DHB-SRI shown in Fig. 1 consists of three switches and two resonant LC tanks. The resonant inductors, called work coil, of the resonant LC tanks are induction heating elements placed underneath a conductive cooking vessel with a thermal insulator between them and have the forms of flat disc with litz wire.

Fig. 2 shows two half bridge series resonant inverters to operate each work coil. To heat up the cooking vessel over the work coil L_{r1}, the first half bridge series resonant inverter, HB1, composed of S_1, S_3, L_{r1} and C_{r1}

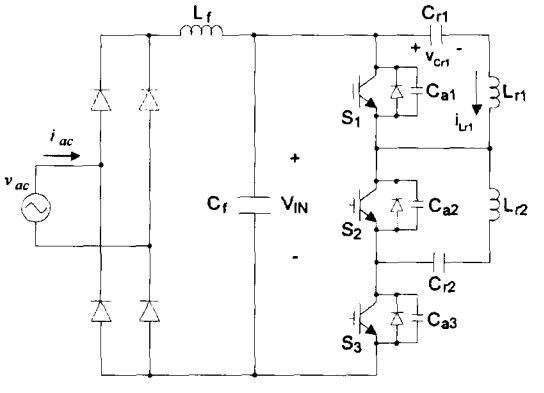

Fig. 1 The proposed Dual Half Bridge Series Resonant Inverter (DHB-SRI)

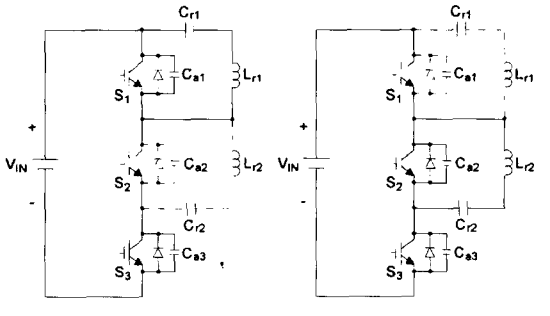

Fig. 2 Two half bridge series resonant inverters

as shown in Fig. 2(a) is activated under the condition that S_2 turns on. Similarly, the second half bridge series resonant inverter, HB2, formed by S_2, S_3, L_{r2} and C_{r2} as shown in Fig. 2(b) operates under the condition that S_1 turns on. In this sense, the proposed circuit is named DHB-SRI.

3. MODE ANALYSIS

For simplicity of the explanation, I assume that all the switching devices and the resonant components are ideal. Since the switching time is short, the rectified voltage, VIN, at twice the line frequency is regarded as the constant voltage source during the switching period. Under these assumptions, the six mode diagrams of the HB1 operation are shown in Fig. 3 and related waveforms are depicted in Fig. 4.

Mode 1 (t_1~t_2) : At the initial condition, S_1 is in off-state and the work coil current, i_{Lr1}, flows through the antiparallel diodes of S_2 and S_3. If S_3 is turned on in advance with zero voltage condition, this mode starts at the changing point of the direction of the work coil current. Then, the resonance between L_{r1} and C_{r1} occurs and the work coil current, i_{Lr1}, increases resonantly.

Before half a resonant period elapses, this mode ends in consequence of turning off S_3 with zero voltage condition.

Mode 2 (t_2~t_3) : This period is an auxiliary resonant mode to attain the zero voltage switching characteristic of the switch S_3. The auxiliary capacitors, C_{a1} and C_{a3}, are discharged and charged by the auxiliary resonance among L_{r1}, C_{r1}, C_{a1} and C_{a3}, respectively. When the Ca1 voltage is zero, the operational state is transferred from here to Mode 3.

Mode 3 (t_3~t_4) : In this mode, the main resonance between L_{r1} and C_{r1} continues through the antiparallel diode of S_1, until the work coil current, i_{Lr1}, becomes zero. Since the S_1 voltage is zero, S_1 is turned on with zero voltage condition in this period.

Mode 4 (t_4~t_5) : The main resonance between L_{r1} and C_{r1} still continues through S_1 and the work coil current, i_{Lr1}, increases resonantly with the reverse direction at

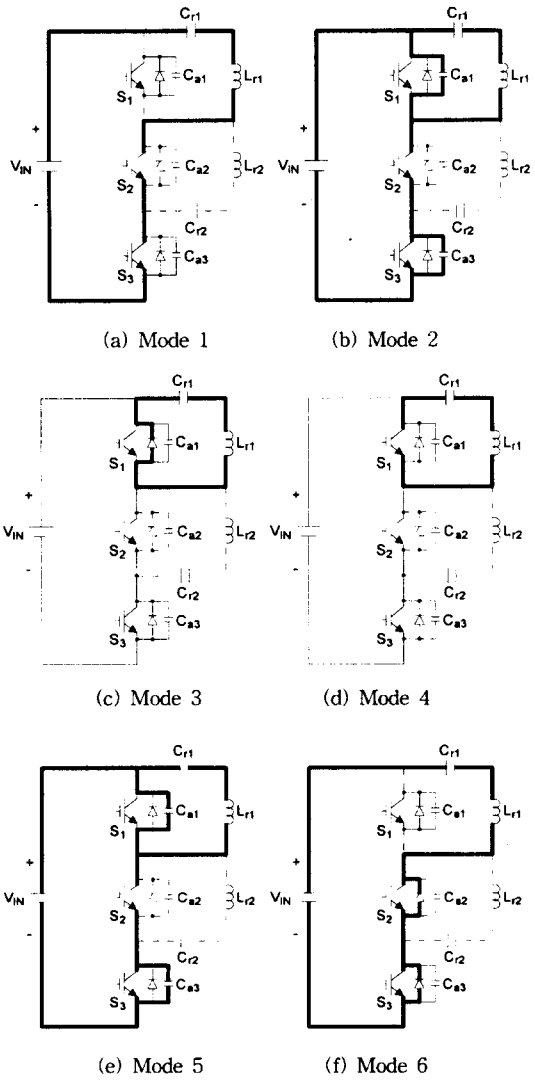

Fig. 3 The six mode diagrams of the HBI operation

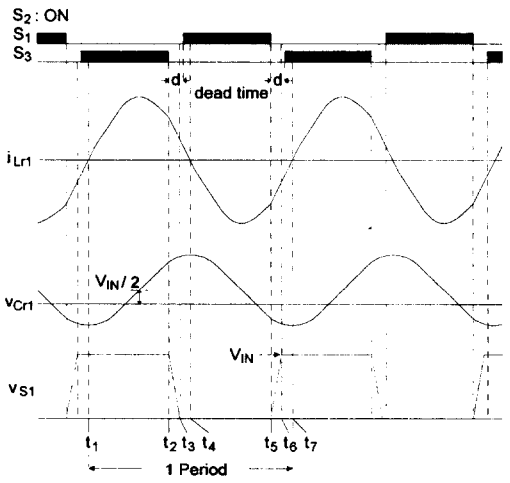

Fig. 4 The typical waveforms of the HB1 operation

Mode 1. If the fixed time determined by switching frequency elapses, S_1 is turned off with zero voltage condition at the end of this mode.

Mode 5 (t_5~t_6) : This mode is the second auxiliary resonant period like Mode 2. The C_{a1} voltage increases from zero to VIN and the C_{a3} voltage decreases from VIN to zero. S_1 can be turned off with zero voltage state by this operation.

Mode 6 (t_6~t_7) : The main resonance between L_{r1} and C_{r1} happens through the antiparallel diodes of S_2 and S_3. In this mode, S_3 is previously turned on under zero voltage condition. One period operation of HB1 is completed at the end of this mode.

For the HB2 operation, under the condition that S_1 is in on-state, S_2 and S_3 are forced to act according to the aforementioned switching procedure.

Table 1 shows the voltage and current equations of the resonant components at each mode. In this table, the initial current $I(0)=i_{Lr1}(0)$ and the initial voltage $V(0)=v_{Cr1}(0)$ are the latest values of the previous mode. The angular frequencies, ω_n and ω_a, of the main resonant modes and the auxiliary resonant modes are expressed by the following equations, respectively.

$$\omega_n = \sqrt{\frac{1}{L_{r1}C_{r1}} - \left(\frac{R}{2L_{r1}}\right)^2} \tag{1}$$

$$\omega_a = \sqrt{\frac{1}{L_{r1}C_p} - \left(\frac{R}{2L_{r1}}\right)^2} \tag{2}$$

where R is the AC resistance of the work coil with load. Assuming that $C_{a1}=C_{a2}=C_{a3}=C_a$, the C_P is expressed by

$$C_p = \frac{C_{r1}\cdot C_a}{C_{r1}+C_a} \tag{3}$$

4. LOSS ANALYSIS

To obtain the proper choice of the cooling system such as a heat sink, a fan and so forth, I have analyzed some losses in this section. The major loss generating parts are classified into work coil, IGBT and bridge diode.

Table 1 The governing equations of each mode

Mode	Governing equations of each mode
Mode 6 ~ Mode 1	$i_{Lr1}(t)=e^{-\frac{R}{2L_{r1}}t}\left\{I(0)\cos\omega_n t+\left(\frac{V_{IN}-V(0)}{L_{r1}}-\frac{R}{2L_{r1}}I(0)\right)\frac{1}{\omega_n}\sin\omega_n t\right\}$ $v_{Cr1}(t)=V_{IN}-e^{-\frac{R}{2L_{r1}}t}\left\{(V_{IN}-V(0))\cos\omega_n t+\left(\frac{R}{2L_{r1}}(V_{IN}-V(0))-\frac{I(0)}{C_{r1}}\right)\frac{1}{\omega_n}\sin\omega_n t\right\}$
Mode 2	$i_{Lr1}(t)=e^{-\frac{R}{2L_{r1}}t}\left\{I(0)\cos\omega_a t+\left(\frac{V_{IN}-V(0)}{L_{r1}}-\frac{R}{2L_{r1}}I(0)\right)\frac{1}{\omega_a}\sin\omega_a t\right\}$ $v_{Cr1}(t)=V(0)+\frac{C_P}{C_{r1}}(V_{IN}-V(0))$ $-e^{-\frac{R}{2L_{r1}}t}\left\{\frac{C_P}{C_{r1}}(V_{IN}-V(0))\cos\omega_a t+\left(\frac{R}{2L_{r1}}\frac{C_P}{C_{r1}}(V_{IN}-V(0))-\frac{I(0)}{C_{r1}}\right)\frac{1}{\omega_a}\sin\omega_a t\right\}$ $v_{Ca1}(t)=V_{IN}-\frac{C_P}{2C_a}(V_{IN}-V(0))$ $+e^{-\frac{R}{2L_{r1}}t}\left\{\frac{C_P}{2C_a}(V_{IN}-V(0))\cos\omega_a t+\left(\frac{R}{2L_{r1}}\frac{C_P}{2C_a}(V_{IN}-V(0))-\frac{I(0)}{2C_a}\right)\frac{1}{\omega_a}\sin\omega_a t\right\}$ $v_{Ca3}(t)=V_{IN}-v_{Ca1}(t)$
Mode 3 ~ Mode 4	$i_{Lr1}(t)=e^{-\frac{R}{2L_{r1}}t}\left\{I(0)\cos\omega_n t-\left(\frac{V(0)}{L_{r1}}+\frac{R}{2L_{r1}}I(0)\right)\frac{1}{\omega_n}\sin\omega_n t\right\}$ $v_{Cr1}(t)=e^{-\frac{R}{2L_{r1}}t}\left\{V(0)\cos\omega_n t+\left(\frac{R}{2L_{r1}}V(0)+\frac{I(0)}{C_{r1}}\right)\frac{1}{\omega_n}\sin\omega_n t\right\}$
Mode 5	$i_{Lr1}(t)=e^{-\frac{R}{2L_{r1}}t}\left\{I(0)\cos\omega_a t-\left(\frac{V(0)}{L_{r1}}+\frac{R}{2L_{r1}}I(0)\right)\frac{1}{\omega_a}\sin\omega_a t\right\}$ $v_{Cr1}(t)=\frac{C_P}{2C_a}V(0)+e^{-\frac{R}{2L_{r1}}t}\left\{\left(1-\frac{C_P}{2C_a}\right)V(0)\cos\omega_a t+\left(\frac{R}{2L_{r1}}\left(1-\frac{C_P}{2C_a}\right)V(0)+\frac{I(0)}{C_{r1}}\right)\frac{1}{\omega_a}\sin\omega_a t\right\}$ $v_{Ca1}(t)=\frac{C_P}{2C_a}V(0)-e^{-\frac{R}{2L_{r1}}t}\left\{\frac{C_P}{2C_a}V(0)\cos\omega_a t+\left(\frac{R}{2L_{r1}}\frac{C_P}{2C_a}V(0)+\frac{I(0)}{2C_a}\right)\frac{1}{\omega_a}\sin\omega_a t\right\}$ $v_{Ca3}(t)=V_{IN}-v_{Ca1}(t)$

Others are of a smaller quantity. Using the induced equations of the previous section, each loss can be calculated by computer simulation with measured data.

1) Bridge Diode Loss (P_d) : Assuming that the power factor of the input line is unity, this loss can be expressed as follows :

$$P_d = i_{d,rms}\cdot V_F \times 2 = \frac{P_{IN}}{V_m/\sqrt{2}}\cdot V_F \times 2 \tag{4}$$

where V_F is the forward voltage of diode, P_{IN} is the input power and V_m is the peak value of the input voltage.

2) IGBT Loss : As IGBT loss, there are switching and conduction losses. Also, the switching loss comprises turn-on loss and turn-off loss. Because the turn-on loss can be neglected in the proposed circuit, the switching loss can be approximated as follows :

$$P_{sw} = \frac{1}{T_i}\sum_{n=1}^{T_i/T_{sw}}\frac{i_{C,n}^2\cdot t_{off}^2}{48\cdot C_a} \tag{5}$$

where i_C and toff are the collector current and the turn-off time of IGBT, respectively and T_i and T_{sw} are a period of the rectified voltage and the switching

Table 2 Calculated losses

	Calculated Loss
Bridge Diode	36.5[W]
IGBT (3 EA)	73.7[W]
Work Coil	56.8[W]
SMPS	12.0[W]
Filter Inductor	18.0[W]
Fan	6.0 [W]
Others	10.0[W]
Total Loss	213[W]

- Input Power=2,800[W]
- Output Power=2,587[W]
- Calculated Efficiency=92.4[%]
- Measured Efficiency=92.0[%]

frequency.

To evaluate the conduction losses of the three switches, a manufacturer specified model that includes an offset voltage(V_{offset}) in series with a resistance(R_S) is employed. Thus, the conduction loss is written as

$$P_{con} = \frac{1}{T_i}\int_0^{T_i}(V_{offset} + R_S i_C)\cdot i_C dt \tag{6}$$

3) Work coil Loss (PWC) : The effective series resistance (ESR) loss mainly comes from the work coil and in most cases the capacitor loss can be neglected. Hence, the ESR loss is expressed as follows :

$$P_{WC} = \frac{1}{T_i}\int_0^{T_i} i_{Lr1}^2 \cdot R_{AC} dt \tag{7}$$

where RAC is the measured AC resistance of the work coil without cooking vessel. Table 2 shows the calculated losses using the above equations. The IGBT loss is the largest one among them and the work coil loss is second. As can be seen in this table, these three parts account for about 80% of the total loss. In this case, the calculated efficiency is 92.4% and the measured efficiency is 92%. Therefore, the calculated value using the above equations nicely coincide with the experimental result. In this case, the efficiency has been calculated by converting the measured temperature change of the water into the transfered power to the load.

5. INPUT FILTER DESIGN FOR THE POWER FACTOR CORRECTION

In order to extract the high power from the outlet, it is essential for the induction heating appliance to have the high power factor capability. Moreover, the system has the compact size and low cost. Thus, a small size LC filter is generally used instead of a large electrolytic capacitor. The LC filter plays the role of the power factor correction.[6]

To obtain the high power factor using the small size LC filter, there are two conditions. First, the resonant frequency f_f of the LC filter should be placed the range as follows :

$$f_{IN} \times 10 < f_f < f_L / 10 \tag{8}$$

where f_{IN} is the frequency of the rectified voltage and f_L is the operating frequency of the proposed inverter, 20~50kHz. This condition should be satisfied so that

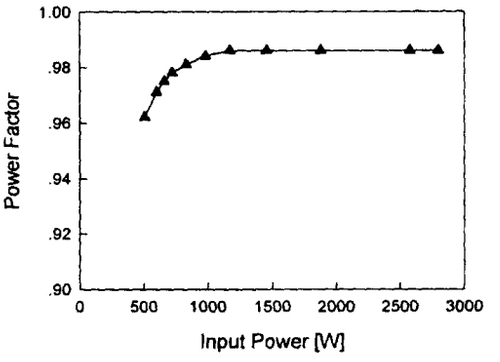

Fig. 5 The power factor according to the input power

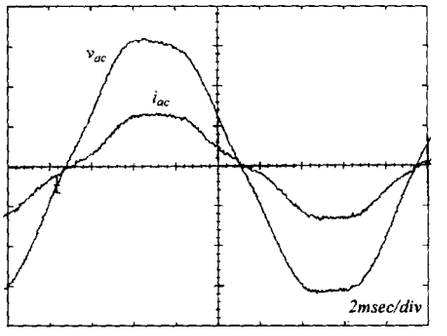

Fig. 6 Experimental waveforms of the input voltage (100V/div) and current (10A/div)

the filter capacitor voltage may follow the rectified voltage well without distortion, and the influence of the LC filter on the inverter operation can be minimized.

The second condition is that the impedance of the LC filter Z_f should be equalized with the load impedance Z_L to attain the high power factor. At this point, each impedance can be calculated as follows :

$$Z_f = \sqrt{L_f / C_f} \tag{9}$$

$$Z_L = \frac{V_m^2}{2P_{IN}} \tag{10}$$

Using the above conditions, the values of the LC filter can be determined. Fig. 5 shows the power factor according to the input power. At the rated power, the power factor is almost 0.99. Fig. 6 shows the experimental waveforms of the input voltage and current when the input power is 2kW. As can be seen in this figure, they agree with the previous explanations.

6. DESIGN PROCEDURE OF RESONANT COMPONENTS

In the series resonant inverter, there are two control methods of the output power such as above- and below-resonance controls. In general, the above- resonance control method is utilized in the induction heating cooker to obtain the high frequency ZVS(Zero Voltage Switching) property and to minimize the audible noises. As can be seen in Fig. 7, the output power according to the operating frequency has the Gaussian-Distribution curves centering at the resonant frequency. Thus, setting the resonant frequency to 20kHz, the output power can be controlled by varying the operating frequency in the range of 20kHz to 50kHz.

1) Work Coil : To design the resonant components, the specification of the available switches in the market should be considered first of all. Then, the proper current rating (I_{WC}) of the work coil can be chosen. Considering the skin effect at the operating frequency, the diameter of one wire can also be selected using the wire table. Setting the current density (J_{WC}) in the wire to 6~8[A/mm^2], the number of wire strands (N_{WC}) can be expressed by :

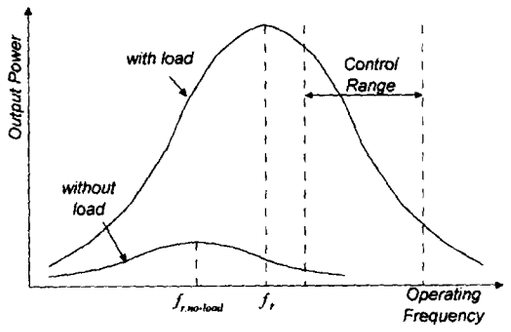

Fig. 7 The output power characteristic curves according to the operating frequency

$$N_{WC} = \frac{I_{WC}}{\pi(D/2)^2 \cdot J_{WC}} \tag{11}$$

where D is the diameter of one wire. Because the diameter of the work coil is fixed, the number of turns in the work coil are easily chosen. The work coil has been built by the aforementioned design procedure, and the measured inductances of the work coil are 72[μH] and 38[μH] without and with cooking vessel, respectively.

2) Main Resonant Capacitor : Once the work coil is designed, the main resonant capacitor can be easily selected by setting the resonant frequency to 20kHz. Through the simulation with the derived governing equations of each mode in the previous section, the other ratings of the capacitor can be determined.

3) Auxiliary Resonant Capacitor : The auxiliary resonant capacitors are used to minimize the turn-off switching losses of the switching devices. Thus, these capacitors should be sufficiently enlarged on the ground

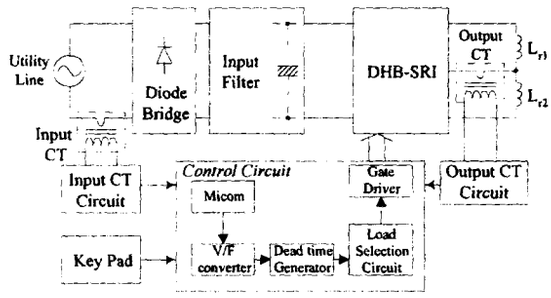

Fig. 8 The block diagram of the control circuit of the proposed DHB-SRI

of the equation (5). However, in order to minimize an bad effect such as the change of the main operating frequency, the deviation of the ZVS condition and so on, these are designed less than one-tenth of the main resonant capacitor.

7. EXPERIMENTAL RESULTS

To verify the above mentioned operation of the proposed DHB-SRI, the proto-type circuit with 230V 2.8kW power consumption for each work coil as shown in Fig. 8 is built and tested. Each work coil inductance is 72[μH] and 38[μH] without and with cooking vessel, respectively. The others are $C_r=C_{r1}=C_{r2}=1.5[\mu F]$, $C_a=C_{a1}=C_{a2}=C_{a3}=47[nF]$, $C_f=5[\mu F]$ and $L_f=0.5[mH]$.

Fig. 9 and Fig. 10 show the work coil current i_{Lr1} and

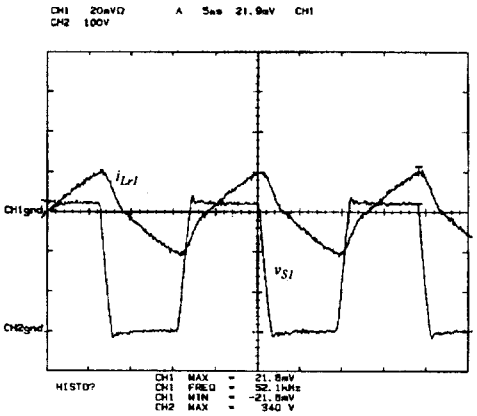

Fig. 9 Work coil current i_{Lr1} (20A/div) and switch voltage v_{S1} (100V/div) at minimum power

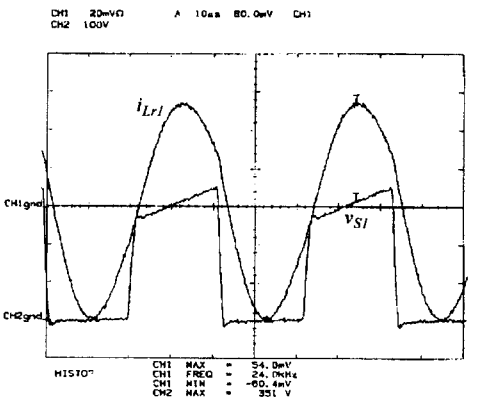

Fig. 10 Work coil current iLr1 (20A/div) and switch voltage vS1 (100V/div) at full power

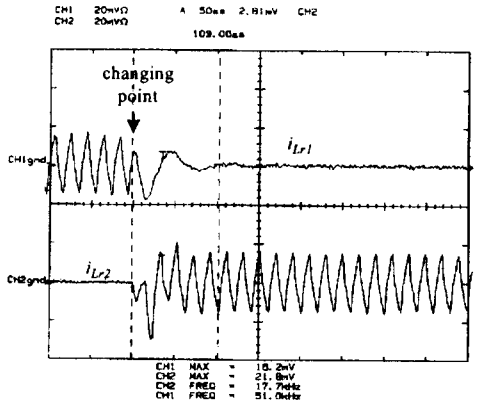

Fig. 11 The current waveforms (20A/div) of the two work coils when the loads are changed

the S_1 switch voltage v_{S1} at the minimum and rated powers, respectively. They are in accord with the aforementioned explanation of the HB1 operation. If two cooking vessels are heated up at the same time, HB1 and HB2 should be operated by turns after the operating time is divided into two in proportion to each power. In the case, the current waveforms of the two work coils at the changing point of two loads are shown in Fig. 11. As can be seen in this figure, the settling time is about 100[μsec]. Thus, the proposed circuit is capable of not only minimizing the changing time of two loads but also maximizing the power utilization capability. Moreover, any acoustic noises except for the small fan noise have not been occurred because only one work coil is operated at a moment.

8. CONCLUSION

In this paper, the new high power factor Dual Half Bridge Series Resonant Inverter (DHB-SRI) for an induction heating appliance with multiple loads is proposed. Because the two loads can be operated in turn using the proposed circuit, the acoustic noise caused by the difference between operating frequencies of adjacent loads can be eliminated. Moreover, the circuit enables independent full power range control of two loads by one inverter circuit and has the zero voltage switching characteristic to obtain the minimum loss and the high frequency switching capability. The

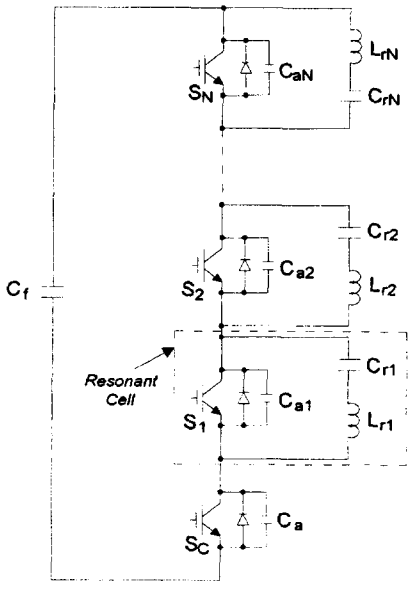

Fig. 12 The half bridge series resonant inverter with multiple loads

operational principle and the mode analysis of the proposed DHB-SRI are presented. According to the loss analysis, I confirm that the DHB-SRI has good efficiency. The input filter design method is suggested not only to get the high power factor correction capability but also to reduce the total system size. The design procedures of the work coil and the resonant capacitors are also presented. Using the designed values, the proto-type circuit with 2.8kW power consumption for each induction heating element is built and tested. Through the experimental results, the performances of the proposed circuit are verified.

In this paper, the proposed circuit can operate the two loads in turn at the same time. On the other hand, the half bridge series resonant inverter with multiple loads as shown in Fig. 12 is very useful in case that it is necessary to heat up more than three cooking vessels simultaneously. The circuit consists of a common switch and multiple resonant cells, and is also compounded of the half bridge series resonant inverters which equal the number of loads like DHB-SRI. In this case, to control the power of each load, each half bridge series resonant inverter should be operated by turns after the operating time is divided in proportion to each power of load. Consequently, the proposed circuit is a very attractive method since the multiple cooking vessels can be worked by one simple inverter circuit.

REFERENCES

[1] L. Hobson, D. W. Tebb and D. Turnbull, "Dual-element Induction Cooking Unit Using Power MOSFETs", International Journal of Electronics, Vol. 59, No. 6, pp.747~757, 1985.

[2] H. Omori and M. Nakaoka, "New Single-ended Resonant Inverter Circuit and System for Induction-Heating Cooking Apparatus", International Journal of Electronics, Vol. 6, No. 2, pp.277~296, 1989.

[3] H. W. E. Koertzen, J. A. Ferreira and J. D. van Wyk, "A Comparative Study of Single Switch Induction Heating Converters Using Novel Component Effectivity Concepts", IEEE Industry Applications Society Conference Rec., pp.298~305, 1992.

[4] H. W. E. Koertzen, J. A. Ferreira and J. D. van Wyk, "Design of the Half-Bridge, Series Resonant Converter for Induction Cooking", IEEE Power Electronics Specialists Conference, pp.729~735, 1995.

[5] Jih-Sheng Lai, Don Hurst and Tom Key, "Switch-Mode Power Supply Power Factor Improvement via Harmonic Elimination Methods", IEEE Applied Power Electronics Conference, pp.415~422, 1991.

〈저 자 소 개〉

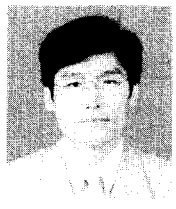

정용채(鄭龍采)

1966년 2월 28일생. 1989년 2월 한양대학교 전자공학과 졸업. 1991년 2월 한국과학기술원 전기 및 전자공학과 졸업(석사). 1995년 8월 한국과학기술원 전기 및 전자공학과 졸업(공박). 1995년 ~ 현재 LG전자 리빙시스템연구소 전력전자팀 선임연구원.